

# Circ\_NCKAP1 promotes skin basal cell carcinoma progression by sponging the miR-148b-5p/HSP90 axis

Z.-X. FAN, W. XI, X.-Y. MIAO, L.-Y. LI, G.-Y. MIAO

Department of Dermatology, Affiliated Hospital of Hebei University of Engineering, Handan, Heibei, China

*Zhixia Fan was the first author, and Wang Xin was the second author*

**Abstract. – OBJECTIVE:** Skin basal cell carcinoma (BCC) is the most common malignant skin tumor. Recent studies demonstrated that circular RNAs (circRNAs) are implicated in tumorigenesis and may represent potential therapeutic targets. The aim of the present study was to explore the expression profiles of circRNAs and their role in skin BCC.

**MATERIALS AND METHODS:** Three pairs of skin BCC tissues and adjacent tissues were used to perform a circRNA microarray for screening of circRNA expression profiles. Circ\_NCKAP1 was selected as a target circRNA by RT-qPCR verification and bioinformatics analysis. The effect of circ\_NCKAP1 knockdown on cell proliferation and apoptosis was assessed using CCK8 and Annexin V-FITC/PI assays, and its regulation over the miR-148b-5p/HSP90 axis was assessed by dual-luciferase reporter assay.

**RESULTS:** Circ\_NCKAP1 was found to be significantly upregulated in skin BCC tissues ( $p < 0.05$ ). In vitro loss-of-function assays demonstrated that circ\_NCKAP1 knockdown markedly inhibited cell proliferation and promoted cell apoptosis ( $p < 0.05$ ). Moreover, Dual-Luciferase reporter assay identified that circ\_NCKAP1 could bind to miR-148b-5p directly, and HSP90 was targeted by miR-148b-5p.

**CONCLUSIONS:** Circ\_NCKAP1 can promote skin BCC progression by sponging the miR-148b-5p/HSP90 axis, and circ\_NCKAP1 may be a potential target for skin BCC therapy.

*Key Words:*

Cutaneous basal cell carcinoma, Circ\_NCKAP1, MiR-148b-5p, HSP90.

epidermal keratinocytes, accounting for 65-75% of all skin malignancies and 80% of non-melanocytic skin tumors<sup>1</sup>. BCC mainly develops in exposed areas of the skin, with 80% of the cases in the head and neck, and 15% in the trunk and limbs. The incidence of skin BCC continues to increase with advancing age<sup>2</sup>. Skin BCC can manifest in a variety of pathological types, the most common of which is nodular<sup>3</sup>. Others include sclerosing, infiltrative, micronodular, and basosquamous. Skin biopsy and pathological examination is the gold standard for the diagnosis of skin BCC<sup>4</sup>. Treatment options include surgical resection and margin assessment, as well as intralesional chemotherapy, cryotherapy, photodynamic therapy, laser therapy and radiation therapy<sup>5</sup>. The pathogenesis of BCC is complex, and the specific underlying mechanism has yet to be fully elucidated.

Circular RNA (circRNA) is a type of non-coding RNA that is widely expressed in eukaryotic and prokaryotic cells and is characterized by a covalent closed-loop structure<sup>6</sup>. Due to the lack of 5' and 3' free ends, it is not easily degraded by Ribonuclease R (RNase R)<sup>7</sup>; in addition, the majority of circRNAs are highly conserved among different species and exhibit cell type-specific and tissue-specific expression patterns<sup>8</sup>. Previous studies<sup>8-10</sup> have demonstrated that circRNA abnormal expression and regulation are involved in the occurrence and development of a variety of tumors. However, the function and interactions of circRNAs in skin BCC remain unknown. In the present study, human circRNA microarray analysis was used to screen the circRNA expression profiles in skin BCC and identified that circ\_NCKAP1 was significantly upregulated in skin BCC. Loss-of-function assays demonstrated that circ\_NCKAP1 may inhibit cell proliferation and promote cell

## Introduction

Skin basal cell carcinoma (BCC) is the most common skin malignant tumor that originates from

apoptosis. Furthermore, circ\_NCKAP1 was found to act as a competitive endogenous RNA (ceRNA) to sponge miR-148b-5p in order to upregulate the expression of heat shock protein (HSP)90. Our study indicated that the circ\_NCKAP1-miR-148b-5p-HSP90 axis participates in the occurrence and development of skin BCC and circ\_NCKAP1 may be a potential target for BCC therapy.

## Materials and methods

### *Clinical Tissues and Cell Lines*

Three pairs of skin basal cell carcinoma tissues and adjacent tissues were collected from Affiliated Hospital of Hebei University of Engineering. The diagnosis and treatment of skin basal cell carcinoma in our study were followed by NCCN Clinical Practice Guidelines in Oncology: Basal Cell Skin Cancers (2019.v1)<sup>10</sup>. None of the patients received preoperative chemotherapy and radiotherapy. The clinicopathologic characteristics of 3 patients shown in **Supplementary Table I**. Human skin basal cell cancer cell line TE354.T (Item No.: ZQ0046) and the human immortal keratinocyte cell line HaCaT (Item No.: ZQ0047) were purchased from Shanghai Zhong Qiao Xin Zhou Biotechnology Co., Ltd (Shanghai, China). This project was approved by the Ethics Committee of Affiliated Hospital of the Hebei University of Engineering.

### *Reagents*

RPMI-1640 medium, high glucose DMEM, and trypsin were purchased from Gibco Co., Ltd (Thermo Fisher Scientific, Waltham, MA, USA). The Dual-Luciferase detection kit was purchased from Promega Co., Ltd (Madison, WI, USA). Transfection reagent Lipofectamine<sup>3000</sup>™ (Lip3000), M-MLV reverse transcriptase, TRIzol, and Real-Time PCR kit were bought from Invitrogen Co., Ltd (Thermo Fisher Scientific, Waltham, MA, USA). Anti-Hsp90 antibody (ab13495) was purchased from Abcam Co., Ltd (Thermo Fisher Scientific, Waltham, MA, USA). PVDF membrane, CL chemiluminescence kit was purchased from Bio-Rad Co., Ltd (Hercules, CA, USA). The psiCHECK2 dual luciferase reporter gene vector was purchased from Shanghai Hanheng Biotechnology Co., Ltd (Shanghai, China).

### *CircRNA Expression Profiling*

Total RNA was extracted from three pairs of tissues and treated with RNase R (EpicentreTech-

nologies, Inc., Madison, WI, USA) to remove linear RNA, and then amplified with random primers and reverse-transcribed into fluorescence-labeled cRNA (Invitrogen, Inc., Carlsbad, CA, USA). The labeled cRNAs were purified using RNeasy Mini Kit. A total of 1 µg of fluorescence-labeled cRNA was mixed with 5 µl of 10X Blocking Agent, 1 µl of 25X lysate, and 25 µl of 2X hybridization buffer, followed by the addition of 50 µl hybridization reaction solution into the Human Circular RNA Array reaction slide. The hybridization reaction was conducted at 65°C for 17 h. After the reaction was completed, the slides were fixed and scanned on an Agilent G2505C scanner. The Agilent Feature Extraction Software (version 11.0.1.1) (Thermo Fisher Scientific, Inc., TX, USA) was used to analyze the hybrid pictures and extract the data. Finally, the data were normalized and analyzed to identify the differentially expressed circRNAs between the two groups of samples. Fold change and *p*-values were screened, and the t-test was used to select the circRNA with a fold difference of  $\geq 1.5$  and  $p < 0.05$ . circRNAs chip detection and data analysis were undertaken by Shanghai Genechem Co.Ltd (Shanghai, Chinese).

### *Reverse Transcription-Quantitative PCR*

RNA was extracted by TRIzol<sup>®</sup> reagent (Invitrogen, Inc., Carlsbad, CA, USA) and reverse-transcribed to cDNA. The SYBR Green Master Mix (Bio-Rad Laboratories, Inc., Hercules, CA, USA), template, upstream/downstream primers, and ddH<sub>2</sub>O, were prepared into a PCR reaction solution and placed on a Real-time PCR instrument for PCR amplification. The reaction conditions were as follows: Pre-denaturation at 95°C for 2 min, followed by 40 cycles at 95°C for 1 min, 60°C for 1 min, 72°C for 1 min, and extension at 72°C for 7 min. The relative expression levels of target RNAs were quantified using the  $2^{-\Delta\Delta C_q}$  method.

### *Bioinformatics Analysis*

Gene Ontology (GO) database (<http://www.geneontology.org>) was used to perform gene function enrichment analysis of differential circRNA-derived genes. The Kyoto Encyclopedia of Genes and Genomes (KEGG) database (<http://www.genome.jp/kegg/pathway.html>) was used to perform pathway analysis of differential circRNA-derived genes.

### *Cell Transfection*

TE354.T cells were cultured in RPMI-1640 medium supplemented with 10% fetal bovine serum

at 37°C, 5% CO<sub>2</sub>, using saturated humidity incubators. When the degree of cell fusion reached approximately 50%, 50 nmol/l circ\_NCKAP1 siRNA plasmid (si-circ\_NCKAP1) and control siRNA (si-NC) were synthesized by Shanghai Genechem Co.Ltd (Shanghai, Chinese) and transfected into TE354.T cells using Lipofectamine 3000™ according to the instructions of the manufacturer (Thermo Fisher Scientific, Inc., TX, USA). After 48 h of transfection, EDTA-trypsin digestion was performed for subsequent experiments.

### **CCK-8 Assay**

TE354.T cells were collected in 96-well plates at 24, 48, 72 and 96 h after transfection, and five replicates at each time point were performed according to the instructions of the CCK-8 Kit. A total of 20 µl CCK-8 reagent were added and then cultured for 2 h. Optical density (OD) value was measured at 450 nm on a microplate reader (BioTek, Inc., Winooski, VT, USA).

### **Annexin V-FITC/PI Double-Staining Assay**

TE354.T cells in the logarithmic growth phase were collected and resuspended in PBS to 10<sup>6</sup> cells/ml. The cells were then stained with 5 µl AnnexinV-FITC kit (Invitrogen, Inc., Carlsbad, CA, USA) for 15 min and 5 µl propidium iodide (PI) kit (Invitrogen, Inc., Carlsbad, CA, USA) for 20 min. The apoptosis rate was detected by flow cytometry (Becton Dickinson, Inc., Franklin Lakes, NJ, USA).

### **Dual-Luciferase Reporter Assay**

The psiCHECK2 dual-luciferase reporter gene vector (Promega, Inc., Madison, Wisconsin, USA) was purchased from Shanghai Hanheng Biotechnology Co., Ltd. (Shanghai, China). The circ\_NCKAP1 sequence with miR-148b-5p binding was cloned into the psiCHECK2 vector (psiCHECK2- circTCF25-wt/mut). The HSP90 3'UTR containing miR-148b-5p binding site was cloned into the psiCHECK2 vector (psiCHECK2- HSP90-wt/mut). Renilla Luciferase was used as the reporter gene and Firefly luciferase as the internal reference gene. Cells were transfected in groups according to the instructions of Lipofectamine 3000™, and Luciferase activity was measured according to the instructions of the manufacturer (Promega, Inc., Madison, Wisconsin, USA). The luminescence value of Renilla Luciferase gene/firefly Luciferase gene (Rluc/Fluc) was recorded as the relative Luciferase activity.

### **Immunohistochemistry (IHC)**

The tissue was fixed with 4% paraformaldehyde solution, embedded in paraffin, and cut into 5-µm serial sections. The paraffin sections were subjected to xylene dewaxing, gradient ethanol hydration, gradient alcohol, and xylene dehydration. and they were incubated with 5% normal goat serum at room temperature for 20 min, rabbit anti-mouse HSP90 monoclonal antibody (Abcam, Cambridge, UK, ab13495, 1:1000) in a refrigerator at 4°C overnight, and biotinylated goat anti-rabbit IgG secondary antibody at 37°C for 1 h. After washing with PBS for 3 times, the sections were incubated with horseradish peroxidase (HRP)-labeled streptavidin antibody (CST, #7074, 1:3000) at 37°C for 30 min. DAB staining, and neutral balata fixation. Finally, the sections were observed under an inverted microscope (Bio-Rad, Hercules, CA, USA). The brown particles indicated positive expression.

### **Statistical Analysis**

All data were processed by statistic package SPSS 18.0 (SPSS, Inc., Chicago, IL, USA) and GraphPad Prism 8.1 (GraphPad, Inc., La Jolla, CA, USA). The variables of normal distribution are shown as  $\chi^2 \pm s$ . Comparison between two groups was performed with *t*-test, and among multiple samples with one-way analysis of variance followed by Tukey's post hoc test. *p*<0.05 was considered to indicate statistically significant differences. <sup>+</sup>*p*<0.05, <sup>\*\*</sup>*p*<0.01.

## **Results**

### **CircRNA Expression Profiling**

Through circRNA microarray analysis and data normalization, the present study identified 543 tumor-associated differentially expressed circRNAs, including 301 downregulated and 242 upregulated circRNAs. GO and KEGG pathway analyses for 543 significantly differentially expressed circRNAs gene symbols were conducted to predict the potential functions of the circRNAs. The GO biological process (GO-BP) analysis results demonstrated that circRNAs gene symbols were more commonly associated with regulation of chromosome organization (GO:0033044) and membrane-bounded organelle (GO:0043227), among others (Figure 1A). The KEGG pathway analysis results indicated that circRNAs gene symbols were mainly enriched in the Hippo signaling pathway and HSP90/JAK signaling pathway, among others (Figure 1B).

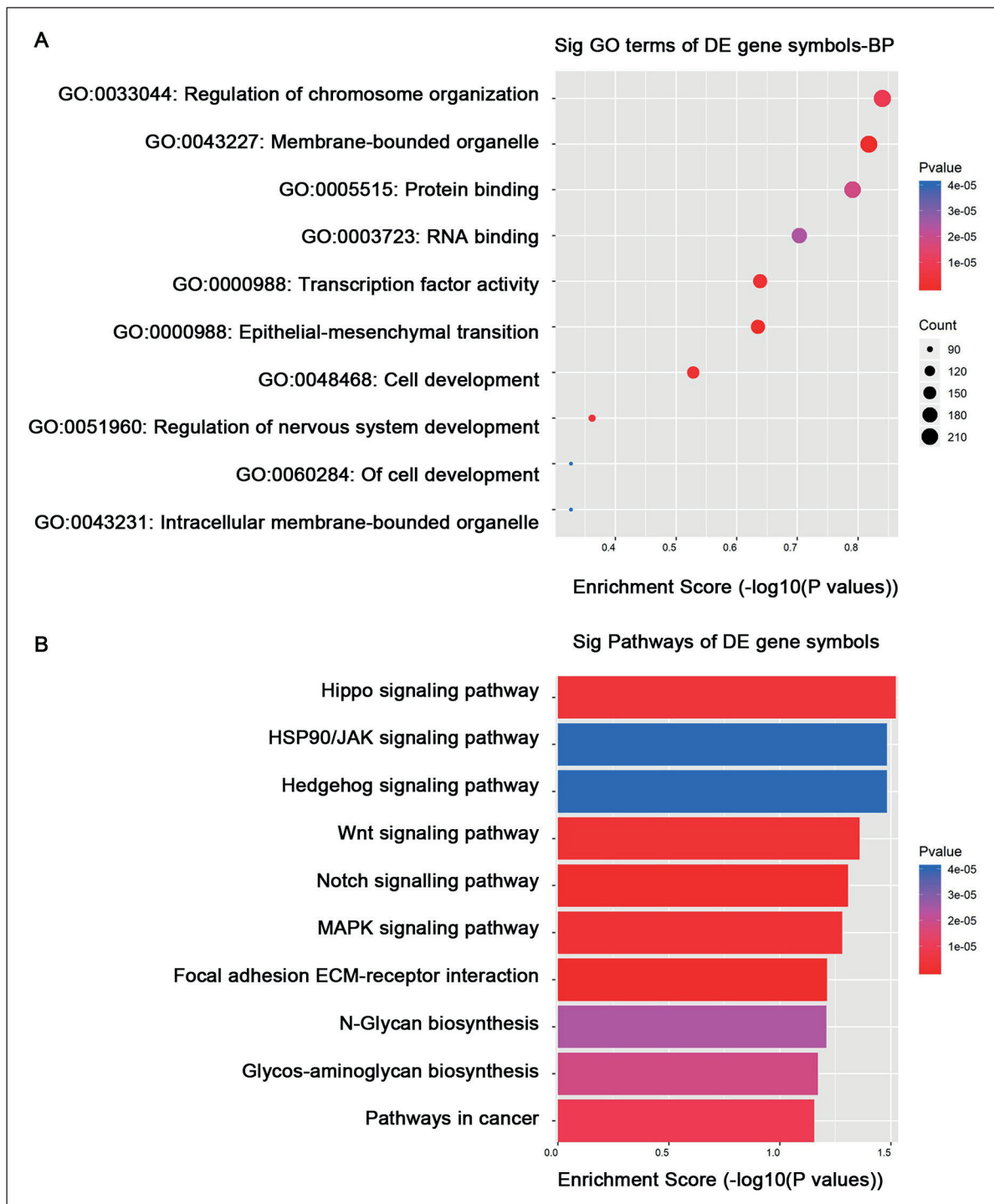


**Figure 1.** Bioinformatics analysis of gene symbols. **A**, GO-BP analysis, the top ten significantly GO-BP terms. **B**, KEGG pathway analysis, the top ten significantly enriched pathways. GO: Gene Ontology, BP: Biological process, KEGG: Kyoto Encyclopedia of Genes and Genomes, DE: Differentially expressed.

***Circ\_NCKAP1 Is Significantly Upregulated in Skin BCC Tissues***

The circRNA microarray data demonstrated that the expression of circ\_NCKAP1 was significantly upregulated in skin BCC tissues (Figure 2A). RT-

PCR assay further confirmed that the expression of circ\_NCKAP1 was significantly upregulated in three pairs of tumor tissues (Figure 2B,  $p < 0.05$ ).



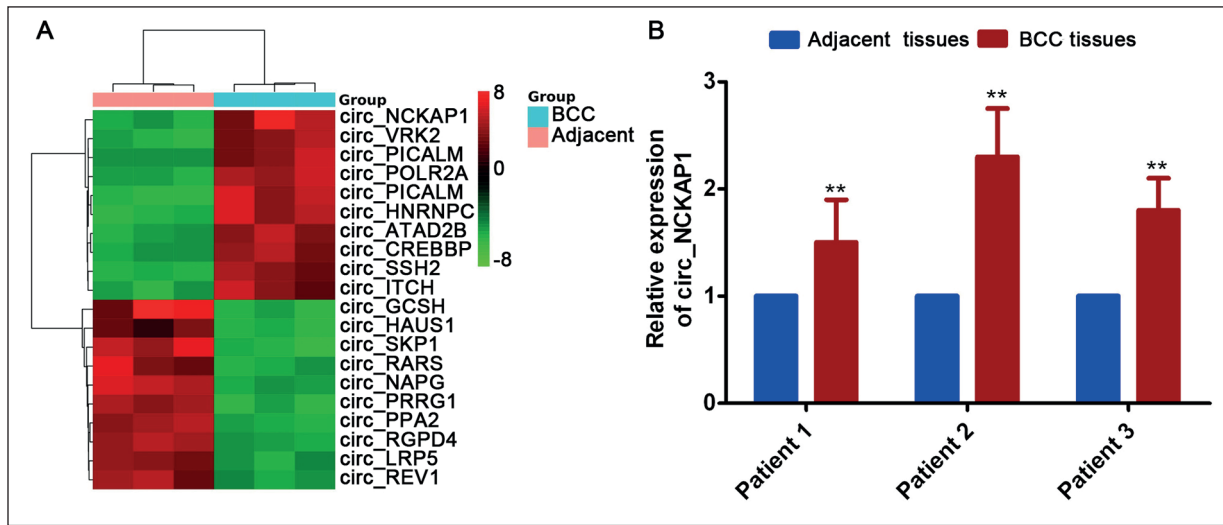


**Figure 2.** circ\_NCKAP1 was significantly upregulated in skin basal cell carcinoma tissues. **A**, Hierarchical cluster map of the top ten differentially expressed circRNAs. **B**, RT-PCR validation was performed using three skin basal cell carcinoma tissues. \* $p < 0.05$ , \*\* $p < 0.01$  compared with adjacent non-cancerous tissues. BCC: Basal cell carcinoma.

### Circ\_NCKAP1 Knockdown Can Inhibit Cell Proliferation and Promote Cell Apoptosis

RT-PCR assay demonstrated that the expression of circ\_NCKAP1 was significantly increased in TE354.T cells, compared with that in HaCaT cells (Figure 3A,  $p < 0.05$ ). circ\_NCKAP1-targeting siRNA expression plasmids were constructed and transfected into TE354.T cells in order to silence circ\_NCKAP1, with si-NC used as a control. RT-PCR assay revealed that the expression of circ\_NCKAP1 in the siRNA group was markedly decreased compared with that in the si-NC group (Figure 3B,  $p < 0.05$ ). In addition, the CKK-8 assay indicated that the absorbance at OD 450 nm in the siRNA group was markedly lower compared

with the si-NC group (Figure 4A,  $p < 0.05$ ), which suggested that circ\_NCKAP1 knockdown inhibited cell proliferation. Annexin V-FITC/PI double-staining assay demonstrated that the apoptotic rate in the siRNA group was significantly lower compared with that in the si-NC group (Figure 4B,  $p < 0.05$ ), which suggested that circ\_NCKAP1 knockdown promoted cell apoptosis.

### Circ\_NCKAP1 Acts as an Endogenous Sponge by Binding MiR-148b-5p

Arraystar's home-made software indicated the putative binding site between circ\_NCKAP1 and miR-148b-5p (Figure 5A). Co-transfection of luciferase reporters containing a wild-type circ\_NCKAP1-3'UTR sequence and miR-148b-

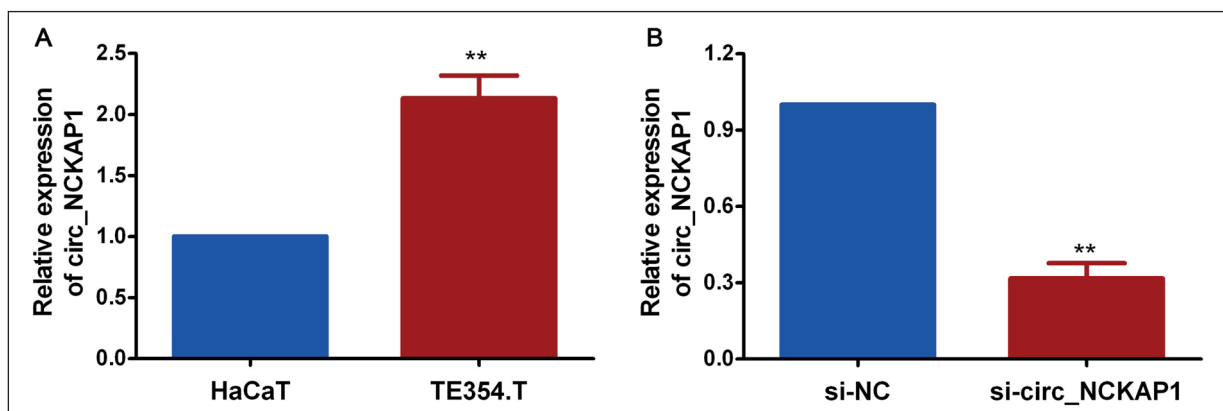


**Figure 3.** siRNA interference. **A**, Expression of circ\_NCKAP1 in TE354.T cells compared with HaCaT cells. \* $p < 0.05$ , \*\* $p < 0.01$ . **B**, The transfection efficiency was detected by RT-PCR. \* $p < 0.05$ , \*\* $p < 0.01$  compared with the si-NC group.

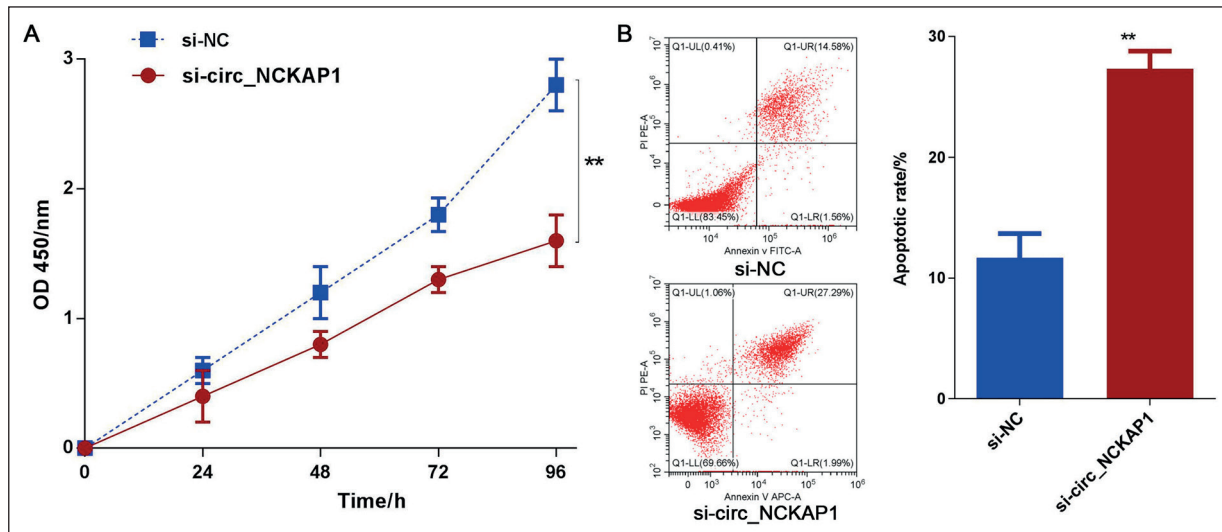


**Figure 4.** Knockdown of circ\_NCKAP1 inhibited cell proliferation and promoted cell apoptosis. **A**, The cell growth rate was measured by the CCK-8 assay. **B**, The cell apoptosis rate was evaluated by Annexin V-FITC/PI double-staining assay. \* $p < 0.05$ , \*\* $p < 0.01$  compared with the si-NC group.

5p mimics into TE354.T cells reduced the luciferase activity to over 50%, but this effect was not observed with co-transfection of the mutant-type circ\_NCKAP1-3'UTR sequence and miR-148b-5p mimics (Figure 5B,  $p < 0.05$ ). Furthermore, RT-PCR analysis demonstrated that the expression of miR-148b-5p was increased in TE354.T cells transfected with si-circ\_NCKAP1, compared with the si-NC group (Figure 5C,  $p < 0.05$ ), and the expression of miR-148b-5p was decreased in skin BCC tissues, compared with adjacent non-cancerous tissues (Figure 5D,  $p < 0.05$ ).

#### HSP90 Is Directly Targeted by MiR-148b-5p

The putative binding sites of miR-148b-5p in the HSP90-3'UTR were predicted by TargetScan and miRanda (Figure 6A), and the results demonstrated that HSP90 is targeted by miR-148b-5p, which was confirmed by dual-luciferase reporter assay (Figure 6B,  $p < 0.05$ ). In addition, the IHC results demonstrated that HSP90 was strongly expressed in skin BCC tissues, and HSP60 was mainly expressed in the cytoplasm of cancer cells, which manifested as light yellow to brown, homogeneous, powdery or granular material (positive), whereas the adjacent non-cancerous tissues were weakly stained or not stained (negative) (Figure 6C,  $p < 0.05$ ). Furthermore, RT-PCR analysis revealed that the expression of HSP90 mRNA was increased in skin BCC tissues, compared with adjacent non-cancerous tissues (Figure 6D,  $p < 0.05$ ).

## Discussion

CircRNAs were first identified in eukaryotic cells in 1979 by HSU<sup>11</sup>, but, it taken into account for recently. Covalently closed circRNAs include three types: Exonic circRNA (ecircRNA), exonic RNA intronic circular RNA (EicircRNA), and circular intronic RNA (ciRNA), and their formation mainly occurs through four pathways: Spliceosome-dependent cyclization, intron-pairing-driven circularization, lasso-driven circularization, and cyclization of protein factor correlation<sup>12</sup>. The specific functions of circRNAs remain unclear, but known functions include miRNA sponging, post-transcriptional regulation, encoding proteins, generating circRNA-derived pseudogenes, and splicing interference<sup>13</sup>. Recent studies have demonstrated that the abnormal expression of circRNAs is implicated in malignant transformation, and may play a significant role in the occurrence and development of several types of human tumors. For example, Dong et al<sup>14</sup> reported that circ\_NT5E can promote non-small-cell lung cancer (NSCLC) cell proliferation by sponging miRNA-134. Yang et al<sup>15</sup> observed that circ\_0001105 can inhibit osteosarcoma progression and metastasis via sponging the miR-766/YTHDF2 axis. Yang et al<sup>16</sup> indicated that Circular RNA-ABCB10 Suppresses Hepatocellular Carcinoma Progression Through Upregulating NRP1/ABL2 via Sponging miR-340-5p/miR-452-5p.

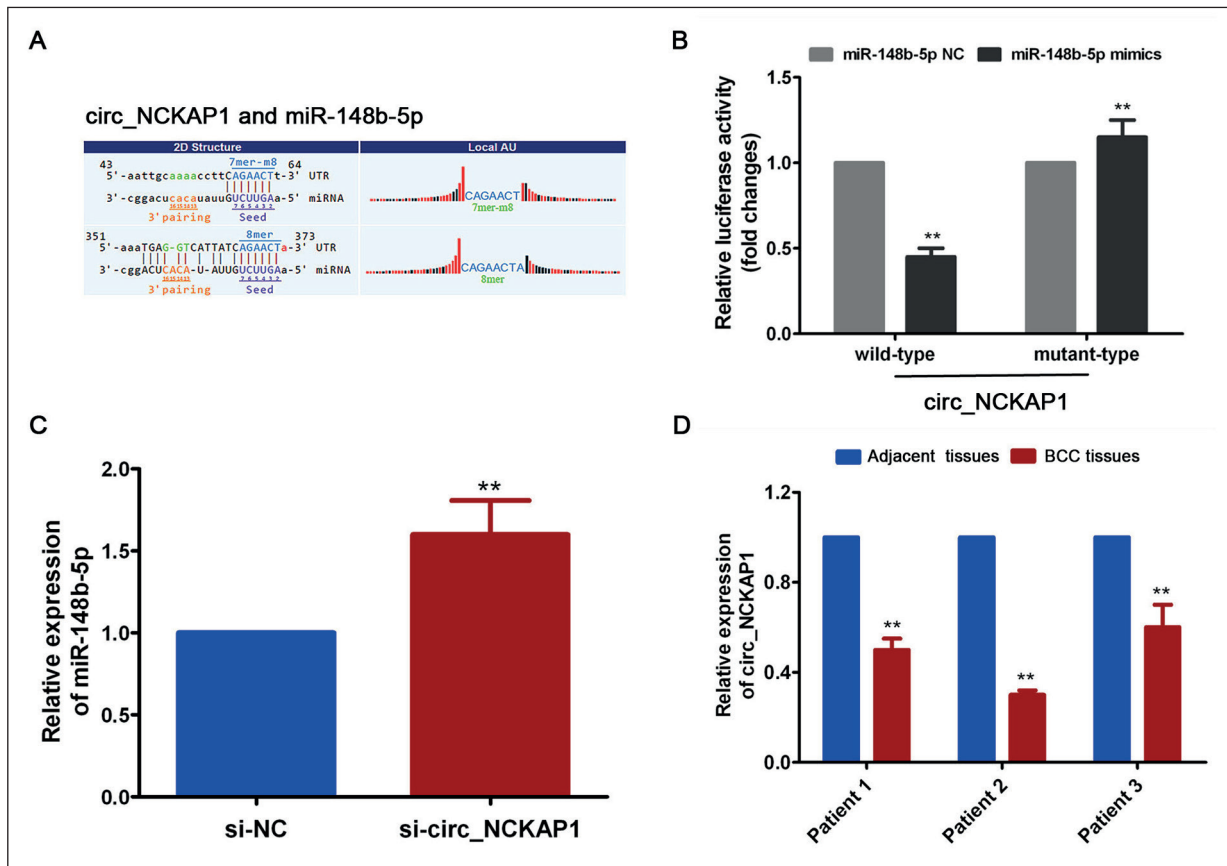


**Figure 5.** Circ\_NCKAP1 acts as an endogenous sponge by binding miR-148b-5p. **A**, Schematic diagram of the binding sites between circ\_NCKAP1 and miR-148b-5p. **B**, Verification of circ\_NCKAP1 targeting miR-148b-5p by dual-luciferase reporter gene assay. **C**, Effect of circ\_NCKAP1 silencing on the expression of miR-148b-5p. \* $p < 0.05$ , \*\* $p < 0.01$  compared with the si-NC group. **D**, The expression of miR-148b-5p in three skin basal cell carcinoma tissues was evaluated by RT-PCR analysis. \* $p < 0.05$ , \*\* $p < 0.01$  compared with adjacent non-cancerous tissues.

In addition, circRNAs are involved in the generation, development and metastasis of several skin tumors. For example, Yang et al<sup>17</sup> found that circ\_Amotl1 can increase the expression of STAT3, DNMT3a and fibronectin through sponging miR-17-5p, thereby accelerating skin wound healing. Zou et al<sup>18</sup> reported that circRNA\_0016418 expedites the progression of human skin melanoma via miR-625/YY1 axis. However, the function and interactions of circRNAs in skin BCC remain elusive. In the present study, the circRNA expression profiles of three skin BCC patients were screened using circRNA microarrays and verified by RT-PCR analysis, and it was observed that circ\_NCKAP1 was significantly upregulated in cancer tissues. The siRNA vector was successfully constructed and transfected into TE354.T cells to silence circ\_NCKAP1 expression. *In vitro* loss-of-function assays demonstrated that circ\_NCK-

AP1 knockdown markedly inhibited cell proliferation and promoted cell apoptosis. Therefore, circ\_NCKAP1 was identified as a key circRNA for skin BCC in this study. Further dual-luciferase reporter assay indicated that circ\_NCKAP1 can function as an endogenous sponge by binding miR-148b-5p to regulate HSP90 expression in skin BCC, and this conclusion was confirmed by RT-PCR and IHC assays.

Circ\_NCKAP1 is an exonic circRNA located in chr2:183817132-183818059, and named hsa\_circRNA\_002092 in the circBase database (<http://www.circbase.org/>)<sup>19</sup>. To the best of our knowledge, this is the first study to investigate the role of circ\_NCKAP1 in cancer. It was recently reported that miR-148b-5p acts as a tumor suppressor in a number of tumors. miR-148b-5p can inhibit gastric cancer metastasis by inhibiting the Dock6/Rac1/Cdc42 Axis<sup>20</sup>, and miR-148b

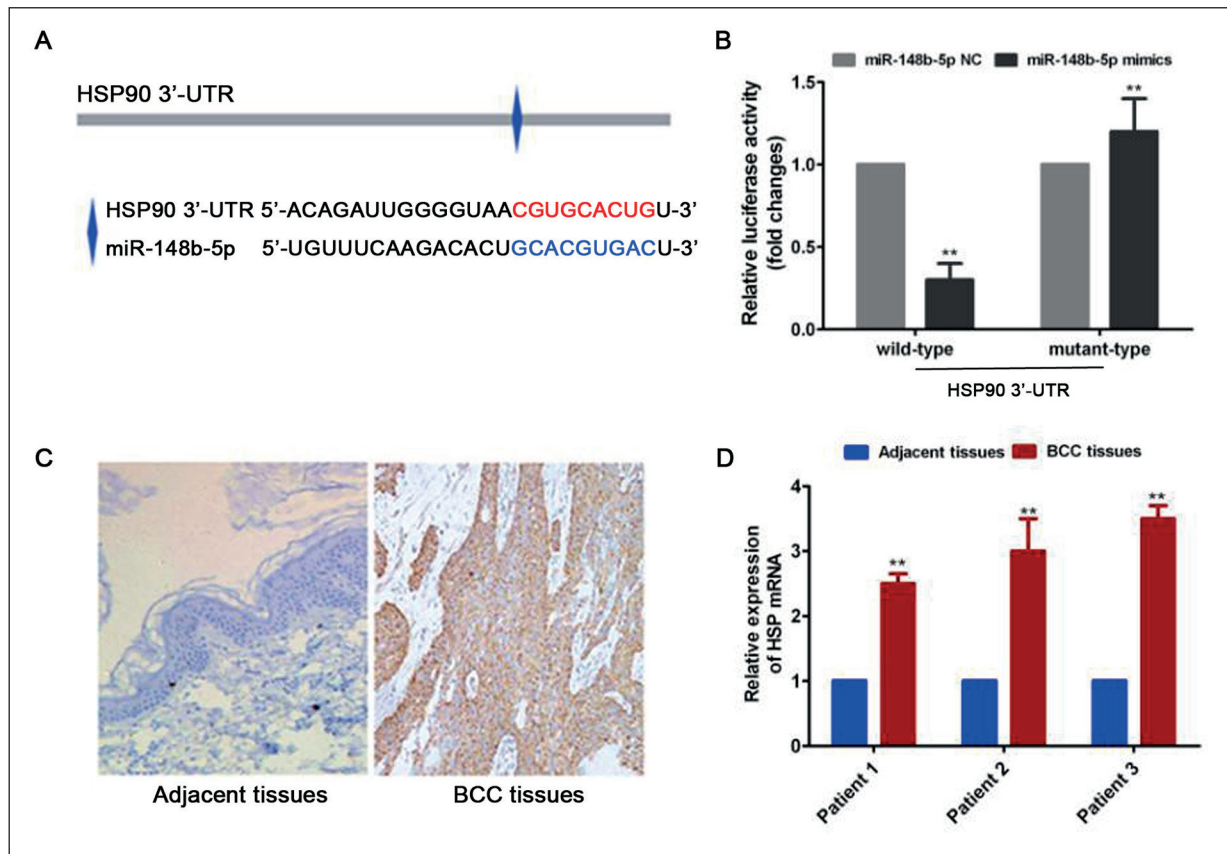


**Figure 6.** HSP90 is directly targeted by miR-148b-5p. **A**, Schematic diagram of the binding sites between HSP90 and miR-148b-5p. **B**, Verification of miR-148b-5p targeting HSP90 by dual-luciferase reporter gene assay. **C**, The expression of HSP90 in skin basal cell carcinoma tissues was analyzed by immunohistochemistry (40 $\times$ ). **D**, The expression of HSP90 mRNA in three skin basal cell carcinoma tissues was assessed by RT-PCR analysis. \* $p$ <0.05, \*\* $p$ <0.01 compared with adjacent non-cancerous tissues. HSP, heat shock protein.

can suppress NSCLC progression by inhibiting ALCAM via the NF- $\kappa$ B pathway<sup>21</sup>. Furthermore, miRNA-148b can enhance the radio sensitivity of B-cell lymphoma cells by targeting Bcl-w to promote cell apoptosis<sup>22</sup>. In the present study, miR-148b-5p was downregulated in skin BCC tissues and may act as a tumor suppressor in skin BCC. Heat shock proteins (HSPs) are a family of highly conserved proteins that are induced by various stressors and their function is to maintain protein stability and promote cell survival<sup>23,24</sup>. They are ubiquitous in organisms<sup>25</sup>, and they are divided into five major families according to their molecular weight: HSP, HSP60, HSP70, HSP90 and HSP100<sup>26</sup>. HSP90 is one of the most common types of HSP in mammals, and it plays an important role in the signal transduction process that promotes tumor cell proliferation and inhibits apoptosis<sup>27,28</sup>. In the present study, HSP90 was

strongly expressed in skin BCC tissues, and may be a new auxiliary tool in the diagnosis or clinical treatment of skin BCC. However, further investigation is required to fully elucidate the role of miR-148b-5p and HSP90 in skin BCC.

The study of circRNAs on skin basal cell carcinoma is very few at present; this was the first report describing the role of circ\_NCKAP1 in skin basal cell carcinoma. Also, to our best knowledge, our study provides the first evidence that circRNAs can regulate the occurrence and development of skin basal cell carcinoma through miRNA sponging. However, for the function of circ\_NCKAP1-miR-148b-5p-HSP90 axis in skin basal cell carcinoma, which requires us to further explore. There were also other limitations to the present study, such as the limited sample size and the lack of *in vivo* animal experiments, which must be addressed in future studies.



## Conclusions

Taken together, the findings of the present study indicated that circ\_NCKAP1 was significantly upregulated in skin BCC tissues, whereas knockdown of circ\_NCKAP1 inhibited cell proliferation and promoted cell apoptosis. Moreover, circ\_NCKAP1 could directly bind to miR-148b-5p, and HSP90 was targeted by miR-148b-5p in skin BCC tissues. Therefore, circ\_NCKAP1 can promote skin BCC progression by sponging the miR-148b-5p/HSP90 axis, and it may be a potential target for the treatment of skin BCC.

## Acknowledgements

This work was supported by important medical funded projects of Hebei province health department (No. zd2013095).

## Conflict of Interest

There are no conflicts of interests and non-financial competing interests in all of authors.

## References

- Rubin AI, Chen EH, Ratner D. Basal-cell carcinoma. *N Engl J Med* 2005; 353: 2262-2269.
- Lewis KD, Fury MG, Stankevich E. Phase II study of cemiplimab, a human monoclonal anti-PD-1, in patients with advanced basal cell carcinoma (BCC) who experienced progression of disease on, or were intolerant of prior hedgehog pathway inhibitor (HHI) therapy. *Ann Oncol* 2018; 29: 23-29.
- Stratigos AJ, Sekulic A, Peris K, Bechter O, Prey S, Kaatz M, Lewis KD, Basset-Seguín N, Chang ALS, Dalle S, Orland AF, Licitra L, Robert C, Ulrich C, Hauschild A, Migden MR, Dummer R, Li S, Yoo SY, Mohan K, Coates E, Jankovic V, Fiaschi N, Okoye E, Bassukas ID, Loquai C, De Giorgi V, Eroglu Z, Gutzmer R, Ulrich J, Puig S, Seebach F, Thurston G, Weinreich DM, Yancopoulos GD, Lowy I, Bowler T, Fury MG. Cemiplimab in locally advanced basal cell carcinoma after hedgehog inhibitor therapy: an open-label, multi-centre, single-arm, phase 2 trial. *Lancet Oncol* 2021; 22: 848-857.
- Russo D, Varricchio S, Iardi G, Martino F, Di Crescenzo RM, Pignatiello S, Scalvenzi M, Costa C, Mascolo M, Merolla F, Staibano S. Tissue Expression of Carbonic Anhydrase IX Correlates to More Aggressive Phenotype of Basal Cell Carcinoma. *Front Oncol* 2021; 11: 659332.
- Cohen PR, Kurzrock R. Basal Cell Carcinoma: Management of Advanced or Metastatic Cancer with Checkpoint Inhibitors and Concurrent Paradoxical Development of New Superficial Tumors. *J Am Acad Dermatol* 2020; 12: 30295-30294.
- Lu Y, Li Z, Lin C, Zhang J, Shen Z. Translation role of circRNAs in cancers. *J Clin Lab Anal* 2021; e23866.
- Zhou Z, Zhang Y, Gao J, Hao X, Shan C, Li J, Liu C, Wang Y, Li P. Circular RNAs act as regulators of autophagy in cancer. *Mol Ther Oncolytics* 2021; 21: 242-254.
- Hatibaruah A, Rahman M, Agarwala S, Singh SA, Shi J, Gupta S, Paul P. Circular RNAs in cancer and diabetes. *J Genet* 2021; 100: 21.
- Verduci L, Tarcitano E, Strano S, Yarden Y, Blandino G. CircRNAs: role in human diseases and potential use as biomarkers. *Cell Death Dis* 2021; 12: 468.
- <https://www.nccn.org/>.
- HSU MT, COCA-PRADOS M. Electron microscopic evidence for the circular form of RNA in the cytoplasm of eukaryotic cells. *Nature* 1979, 280: 339-340.
- Martone J, Mariani D, Desideri F, Ballarino M. Non-coding RNAs Shaping Muscle. *Front Cell Dev Biol* 2020; 7: 394-402.
- Ding L, Wang R, Shen D, et al. Role of noncoding RNA in drug resistance of prostate cancer. *Cell Death Dis* 2021; 12: 590.
- Dong L, Zheng J, Gao Y, Zhou X, Song W, Huang J. The circular RNA NT5E promotes non-small cell lung cancer cell growth via sponging microRNA-134. *Aging (Albany NY)* 2020; 12: 3936-3949.
- Yang J, Han Q, Li C, Yang H, Chen X, Wang X. Circular RNA circ\_0001105 Inhibits Progression and Metastasis of Osteosarcoma by Sponging miR-766 and Activating YTHDF2 Expression. *Onco Targets Ther* 2020; 13: 1723-1736.
- Yang W, Ju HY, Tian XF. Circular RNA-ABCB10 suppresses hepatocellular carcinoma progression through upregulating NRP1/ABL2 via sponging miR-340-5p/miR-452-5p. *Eur Rev Med Pharmacol Sci* 2020; 24: 2347-2357.
- YANG Z, AWAN FM, DU WW. The Circular RNA interacts with STAT3, increasing its nuclear translocation and wound repair by modulating Dnm-t3a and miR-17 function. *Mol Ther* 2017; 25: 2062-2074.
- Zou Y, Wang SS, Wang J, Su HL, Xu JH. CircRNA\_0016418 expedites the progression of human skin melanoma via miR-625/YY1 axis. *Eur Rev Med Pharmacol Sci* 2019; 23: 10918-10930.
- [http://www.circbase.org/cgi-bin/singlerecord.cgi?id=hsa\\_circ\\_002092](http://www.circbase.org/cgi-bin/singlerecord.cgi?id=hsa_circ_002092).
- Li X, Jiang M, Chen D. MiR-148b-3p inhibits gastric cancer metastasis by inhibiting the Dock6/Rac1/Cdc42 axis. *J Exp Clin Cancer Res* 2018; 37: 71-82.
- Jiang Z, Zhang J, Chen F, Sun Y. MiR-148b suppressed non-small cell lung cancer progression via inhibiting ALCAM through the NF- $\kappa$ B signaling pathway. *Thorac Cancer* 2020; 11: 415-425.
- Liu SH, Wang PP, Chen CT. MicroRNA-148b enhances the radiosensitivity of B-cell lymphoma cells by targeting Bcl-w to promote apoptosis. *Int J Biol Sci* 2020; 16: 935-946.

- 23) Milani A, Basirnejad M, Bolhassani A. Heat-shock proteins in diagnosis and treatment: an overview of different biochemical and immunological functions. *Immunotherapy* 2019; 11: 215-239.
- 24) Richter K, Haslbeck M, Buchner J. The heat shock response: life on the verge of death. *Mol Cell* 2010; 40: 253-266.
- 25) Bodzek P, Szymala B, Damasiewicz-Bodzek A, Janosz I, Witek L, Olejek A. Are IgG antibodies to heat shock proteins HSP27 and HSP60 useful markers in endometrial cancer and cervical cancer? *Ginekol Pol* 2021. doi: 10.5603/GP.a2021.0060. Online ahead of print.
- 26) Sun B, Li G, Yu Q, Liu D, Tang X. HSP60 in cancer: a promising biomarker for diagnosis and a potentially useful target for treatment. *J Drug Target* 2021; 1-15.
- 27) Perez C, Rico J, Guerrero C, Acosta O. Role of heat-shock proteins in infection of human adenocarcinoma cell line MCF-7 by tumor-adapted rotavirus isolates. *Colomb Med (Cali)* 2021; 52: e2024196.
- 28) Xu D, Dong P, Xiong Y. MicroRNA-361-Mediated Inhibition of HSP90 Expression and EMT in Cervical Cancer Is Counteracted by Oncogenic lncRNA NEAT1. *Cells* 2020; 9: E632.